ELSEVIER

Journal of Alloys and Compounds 224 (1995) 162–167

Journal of ALLOYS AND COMPOUNDS

Phase structure of V-based solid solutions containing Ti and Ni and their hydrogen absorption–desorption properties

Makoto Tsukahara [a,*], Kunio Takahashi [a], Takahiro Mishima [a], Tetsuo Sakai [b], Hiroshi Miyamura [b], Nobuhiro Kuriyama [b], Itsuki Uehara [b]

[a] *IMRA Material R & D Co., Ltd., 5-50 Hachiken-cho Kariya-shi, Aichi, 448, Japan*

[b] *Osaka National Research Institute, Midorigaoka Ikeda-shi, Osaka, 563, Japan*

Received 15 December 1994; in final form 7 January 1995

Abstract

Crystal structures and pressure–composition isotherms were investigated for the vanadium rich ternary Ti–V–Ni solid solution. The alloy containing more than 85at.% vanadium absorbed hydrogen of 1.6 in H/M ratio that amounted to 3.2 mass% H.

The pressure–composition isotherm for $Ti_{22}V_{66}Ni_{12}$ in the hydrogen pressure range of 10^{0} to 10^{-8} MPa was obtained by the electrochemical method. Two pressure plateaus were found at hydrogen pressures of 10^{-2} MPa and 10^{-6} MPa. The upper plateau would be ascribed to the reaction from dihydride to monohydride and the lower plateau would be ascribed to the reaction from monohydride to solid solution of the alloy and hydrogen.

Keywords: Titanium; Vanadium; Nickels; PCT curves; Hydrogen absorption–desorption

1. Introduction

Vanadium hydrides have been investigated by several authors [1] because of the high mobility of hydrogen at low temperature. A plateau corresponding to the coexistence of $VH_{\sim 0}$ and $VH_{\sim 1}$ appears below the hydrogen pressure of 1 Pa on a pressure–composition isotherm (a PCT curve) at 373 K [2]. This reaction has not been utilized for practical applications because the monohydride is too stable. However, the reaction between $VH_{\sim 1}$ and $VH_{\sim 2}$ has attracted much interest for various kinds of applications such as hydrogen compressors, metal hydride heat pumps and isotope separation [3] because this reaction occurs reversibly under moderate conditions of pressure and temperature. The formation of vanadium dihydride was first reported by Maeland et al. [4]. Reilly and Wiswall [5] measured the PCT curves for the $VH_{\sim 1}$–$VH_{\sim 2}$ system and found that a plateau appears at 0.8 MPa at 327 K.

The crystal structure of vanadium is body centered cubic (bcc). The crystal structure of the monohydride ($VH_{\sim 1}$) was determined to be body centered tetragonal (bct) [6] and that of the dihydride ($VH_{\sim 2}$) to be face centered cubic (fcc) [4]. Vanadium is known to be soluble in various metallic elements in a wide range of composition. The Ti–V system forms solid solution except for more than 97at.% titanium [7]. The phase diagram of the ternary Ti–V–H system shows that the bcc solid solution of $Ti_{1-x}V_x$ ($x > 0.42$) forms the monohydride with the bct structure and the dihydride with the fcc structure [8].

Diffusion rates of hydrogen in bcc metals are extremely high although pure vanadium does not react readily with hydrogen gas to form a hydride. Kleiner et al. [9] reported that the diffusion coefficient of hydrogen atoms in $VH_{<0.7}$ is about 4×10^{-8} m^2 s^{-1} at temperatures from 435 K to 620 K, which is nearly equal to the value in palladium hydride. Therefore the rate determining step was considered to be a surface reaction.

The extremely low hydriding rate of vanadium can be changed by adding some metals to vanadium. According to Maeland et al. [10], a small amount of an additive such as iron, nickel and cobalt enhances the hydriding rate. Libowitz and Maeland [3] investigated the reaction kinetics of hydride formation for various vanadium based alloys, such as V–M (M = Co, Fe, Ni, Cr, Mn) and Ti–V–M (M = Fe, Mn, Cr, Ge, Mn/Fe, Fe/Al, Fe/Si), and discovered conditions for rapid reaction.

* Corresponding author.

SSDI 0925-8388(95)01533-7

In addition to the reaction rate, substitution of some other metals for vanadium also changes other hydriding properties. Kagawa et al. [11] reported the change of dissociation pressure of vanadium hydride by adding titanium and another element such as aluminum, chromium, silicon, etc. They also found that $Ti_{10}V_{90}$ based alloys containing chromium had less pulverizing rate.

When the alloys are applied to a nickel–metal hydride (Ni–MH) battery [12], the addition of nickel would be indispensable from the standpoint of kinetics for electrochemical reaction. The Ti–V–Ni system has also been investigated as one of the promising structural materials for reactors of nuclear fusion and other high temperature applications. The ternary phase diagram for the whole Ti–V–Ni system was reported by Eremenko et al. [13]. However, the hydriding properties of the vanadium rich Ti–V–Ni system have not been reported except for the cases that vanadium content is higher than 70at.% (e.g. Refs. [10,11]).

In the present paper, we report phase diagrams and hydrogen absorption–desorption characteristics of the ternary Ti–V–Ni system in $Ti/V \leqq 1$ and $V/Ni \geqq 1$. A PCT curve for $Ti_{22}V_{66}Ni_{12}$ in the hydrogen pressure range from 10^0 to 10^{-8} MPa has been measured by the electrochemical method [14]. This is the first report that both the upper ($MH_{\sim 2} \rightarrow MH_{\sim 1}$) plateau and the lower ($MH_{\sim 1} \rightarrow MH_{\sim 0}$) plateau are observed on the one PCT curve for a vanadium based alloy.

2. Experimental details

The alloy samples were prepared by arc melting a mixture of the component pure metals of titanium (purity >99%), vanadium (purity >99%) and nickel (purity >99%) on water-cooled copper hearth under 5×10^4 Pa argon gas. Alloy ingots were turned and remelt several times to be homogenized. The surface layer of each ingot was filed off. These as-cast ingots except for the ingots containing a σ-phase were first hydrided at high temperature (<673 K) under high hydrogen pressure (<3.3 MPa) and then mechanically crushed. The alloys containing the σ-phase were mechanically crushed easily without hydriding. X-ray powder diffraction (XRD) analysis by using Cu Kα radiation was conducted on these powder samples degassed under vacuum at 673 K for 4 h. The metallurgical microstructures were examined by scanning electron microscopy (SEM) and electron probe X-ray microanalysis (EPMA).

The PCT curves were measured with a Sieverts' type apparatus. Each powder sample of 0.5–1 g was put in a reactor (SUS316 tube). For the activation of the sample, the reactor was heated to 473–673 K under vacuum, followed by introducing 3.3 MPa hydrogen (purity >99.9999%) into the reactor and then cooling down to room temperature. Just before each run of PCT measurement, the reactor was evacuated at the temperature less than 723 K in order to get a hydrogen zero point.

Electrochemical PCT measurement for the desorption process of $Ti_{22}V_{66}Ni_{12}$ was conducted in a wider pressure range, from 10^0 to 10^{-8} MPa, according to the previous paper [14]. The alloy electrode was prepared by mixing the alloy powder (20 mass% copper-coated) with 10 mass% FEP powder (Daikin Co., tetrafluoroethylene–hexafluoropropylene copolymer) and then by hot-pressing the mixture on a nickel mesh at 573 K. Equilibrium electrode potential vs hydrogen content curves were measured by use of an Hg/HgO reference electrode, a 6M KOH electrolyte and an $Ni(OH)_2$ counter electrode.

3. Results and discussion

3.1. Ti–V–Ni phase diagram

Typical XRD patterns which were obtained from the degassed samples are shown in Fig. 1. According to XRD patterns the ternary Ti–V–Ni alloys with the atomic ratios of $Ti/V \leqq 1$ and $V/Ni \geqq 1$ are divided into six types from A to F as shown in Figs. 1 and 2.

3.1.1. Type A

Binary $Ti_{100-x}V_x$ ($x > 50$) alloys (Fig. 1(a)) were identified as a single bcc phase. This phase is called a β-phase in the present paper as in Eremenko et al. [13]. The binary $Ti_{100-x}V_x$ ($x > 3$) alloys are known to belong to the bcc phase of the (βTi, V) solid solution [7]. A small amount of nickel was able to dissolve in the bcc (βTi, V) solid solution when the titanium content is less than 20at.% (Fig. 2). The alloy composed of the single β-phase is classified into a type A alloy.

3.1.2. Type B and C

When the value of x in $Ti_{10}V_{90-x}Ni_x$ was more than 22, new peaks appeared as shown in Fig. 1(b). This new peak pattern was indexed as a σ-phase cell (CrFe-type structure). The alloys of $Ti_{10}V_{90-x}Ni_x$ ($22 \leqq x \leqq 40$) consisted of the two phases of β and σ, which are labeled as a type B alloy. The alloy of $V_{60}Ni_{40}$ was identified as the single σ-phase as shown in Fig. 1(c), which is labeled as a type C alloy.

3.1.3. Type D

By adding nickel to $Ti_{25}V_{75}$ (β-phase, atomic ratio of $Ti/V = 0.33$), another series of peaks due to the bcc structure was obtained as shown in Fig. 1(d). The composition of the secondary phase was determined to be $TiV_yNi_{\sim 1}$ ($y < 1$) by SEM–EPMA. Each peak due to the secondary phase always appeared at a little

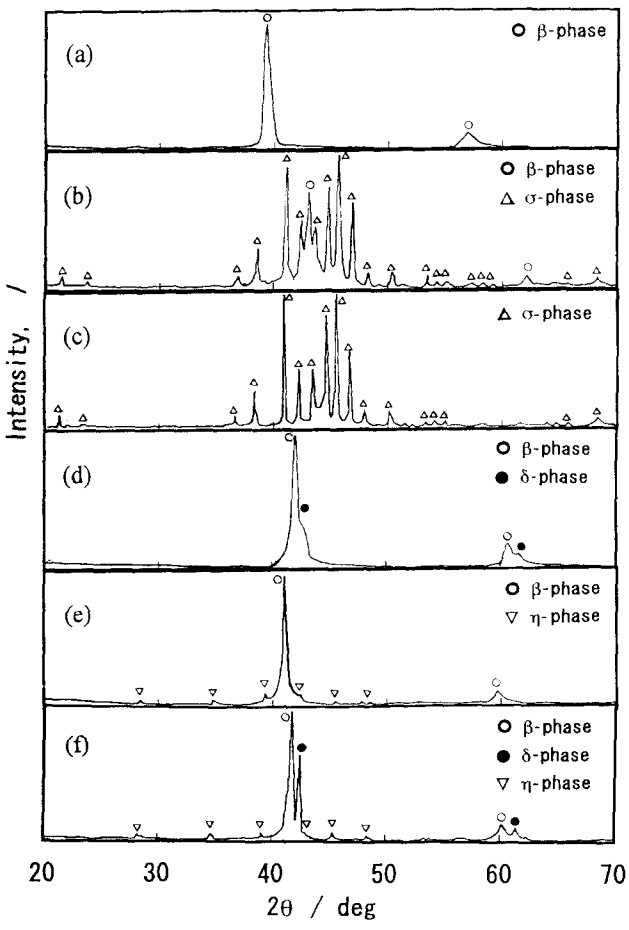

Fig. 1. X-ray (Cu Kα) diffraction patterns of each type of Ti–V–Ni alloys: (a) β-phase ($Ti_{50}V_{50}$); (b) (β+σ)-phases ($Ti_{10}V_{60}Ni_{30}$); (c) σ-phase ($V_{60}Ni_{40}$); (d) (β+δ)-phases ($Ti_{33}V_{57}Ni_{10}$); (e) (β+η)-phases ($Ti_{45}V_{45}Ni_{10}$); (f) (β+δ+η)-phases ($Ti_{40}V_{40}Ni_{20}$).

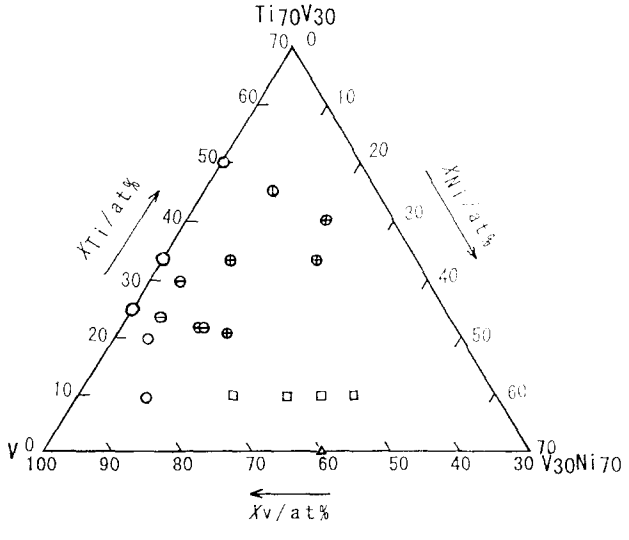

Fig. 2. Classification of the vanadium rich Ti–V–Ni system from the viewpoint of crystal structure. ○; type A (β), □; type B (β+σ), △; type C (σ), ⊖; type D (β+δ), ⊙; type E (β+η), ⊕; type F (β+δ+η).

higher 2θ value than that of the corresponding peak due to the β-phase (Fig. 1(d)), which indicated that the unit cell dimension of the secondary phase were smaller than that of the main β-phase. The TiNi alloy is known to belong to the bcc phase with a ClCs-type structure. This secondary phase would be identified as a solid solution of TiNi and vanadium, which was named a δ-phase by Eremenko et al. [13]. The alloys consisting of (β+δ)-phases are classified into a type D alloy. The δ-phase appeared when more than 6at.% nickel was contained under the atomic ratio Ti/V=0.33 though Eremenko et al. [13] suggested the β/(β+δ) phase boundary was at approximately 15at.% nickel.

3.1.4. Type E and F

By adding nickel to the single β-phase $Ti_{50}V_{50}$ alloy, another XRD pattern was obtained which was indexed as a Ti_2Ni-type structure (Fig. 1(e)). The composition of this secondary phase measured by EPMA was $TiV_{\sim 0}Ni_{\sim 0.5}$, which agreed with the XRD results. This phase was called a η-phase by Eremenko et al. [13]. The alloy with (β+η)-phases is categorized as a type E alloy.

Adding more than 20at.% of nickel, peaks of the δ-phase appeared in addition to peaks of the β-phase and the η-phase (Fig. 1(f)). Therefore the $Ti_{40}V_{40}Ni_{20}$ alloy has three phases of β, δ and η. The alloys with these three phases are labeled as type F alloys.

In the case of $Ti_{21}V_{63}Ni_{16}$ (the atomic ratio of Ti/V=0.33), XRD peaks due to the η-phase were not observed because of the small amount of this phase, but SEM–EPMA showed that the tertiary phase with the composition of $TiV_{\sim 0}Ni_{\sim 0.5}$ existed. This tertiary phase would be the η-phase and this alloy was also classified as a type F alloy (Fig. 2).

Putting these analyses together, the four different phases exist in the ternary Ti–V–Ni system of the composition range of Ti/V≦1 and V/Ni≧1. The four phases are the β-phase (the bcc phase of the (βTi, V) solid solution containing a small amount of nickel), the σ-phase (the CrFe-type structure), the δ-phase (the bcc phase of the TiNi intermetallic compound containing vanadium) and the η-phase (the Ti_2Ni phase containing vanadium with the Ti_2Ni-type structure). According to the combination of these four phases, the alloys are divided into six types as follows: the type A; single β-phase, the type B; (β+σ)-phases, the type C; single σ-phase, type D; (β+δ)-phases, the type E; (β+η)-phases, and the type F; (β+δ+η)-phases. The group classification of these alloys is shown in Fig. 2.

3.2. PCT curves for Ti–V–Ni

PCT curves for the six types of alloys except for the type C (the single σ-phase) were measured with the Sieverts' type apparatus as shown in Figs. 3–6. The

alloy of the type C ($V_{60}Ni_{40}$) was not activated up to 873 K at 5.0 MPa hydrogen.

Fig. 3 shows PCT curves for two alloys of type A. The effect of the atomic ratio of titanium to vanadium on the PCT curves was significant. $Ti_{50}V_{50}$ had no clear plateau, while $Ti_{25}V_{75}$ had a clear plateau. This result is in good agreement with the previous result for $Ti_{40}V_{60}$ [15] that did not have a clear plateau either.

A type B ($\beta+\sigma$) alloy of $Ti_{10}V_{68}Ni_{22}$ was activated under a moderate condition at 473 K at 3.3 MPa hydrogen, showing a rather clear plateau (Fig. 4(a)). On the other hand another type B alloy of $Ti_{10}V_{60}Ni_{30}$ was not activated at 673 K at 3.3 MPa hydrogen but at 873 K at 5.0 MPa hydrogen, and had no clear plateau on its PCT curves as shown in Fig. 4(b). In the former alloy the β-phase was dominant, while in the latter alloy the σ-phase was dominant.

Adding nickel to $Ti_{25}V_{75}$ brought about a lowering of the dissociation temperature in atmospheric pressure, being accompanied by the phase change from the type A (β) to the type D ($\beta+\delta$). As shown in Fig. 5(a), a type D alloy of $Ti_{22}V_{67}Ni_{11}$ (Ti/V=0.33) had a plateau at 0.16 MPa at 353 K, while the type A alloy of $Ti_{25}V_{75}$ (Fig. 3(a), Ti/V=0.33) had a plateau at 0.15 MPa at 433 K. Both of the plateaus were rather clear. Adding nickel to $Ti_{25}V_{75}$ (Type A) brought about the formation of the TiNi-based δ-phase and the enrichment of vanadium content in the main β-phase, which caused the lowering of the dissociation temperature.

As shown in Fig. 5(b), a type E ($\beta+\eta$) alloy of $Ti_{45}V_{45}Ni_{10}$ did not have a clear plateau in a similar manner to observations for $Ti_{50}V_{50}$ (Fig. 3(b)). The pressure plateaus for the coexistence of two hydride phases of these alloys could appear at a pressure lower than 0.01 MPa.

Fig. 6(a) shows a PCT curve for a type F ($\beta+\delta+\eta$) alloy of $Ti_{21}V_{63}Ni_{16}$ (Ti/V=0.33). A clear plateau of this alloy was observed. The dissociation temperature in atmospheric pressure was lower than that of the

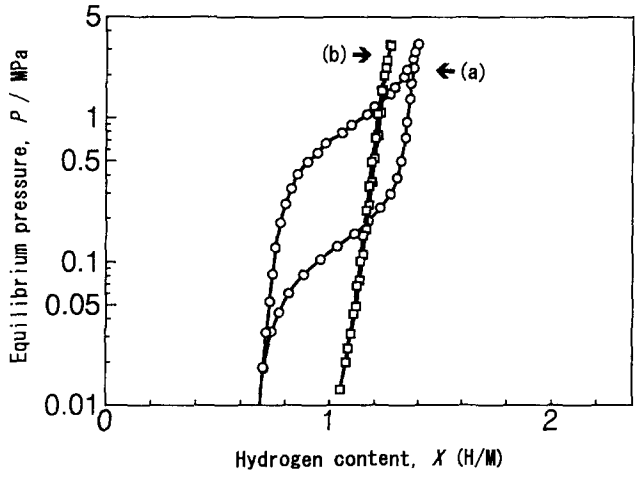

Fig. 3. Typical pressure–composition isotherms for type A alloys of $Ti_{25}V_{75}$ at 433 K (a) and $Ti_{50}V_{50}$ at 573 K (b).

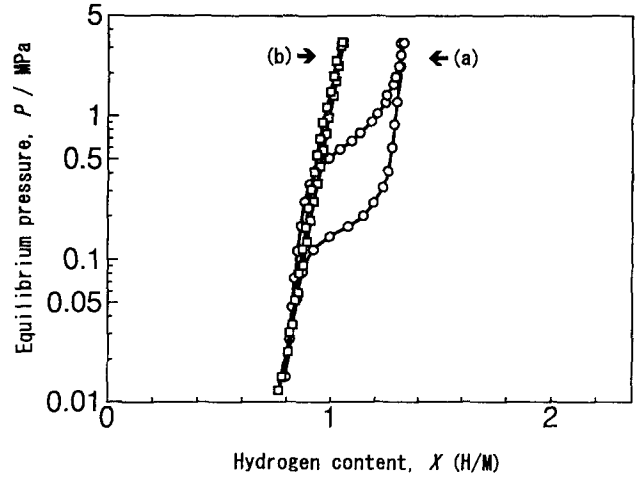

Fig. 5. Typical pressure–composition isotherms for a type D alloy of $Ti_{22}V_{67}Ni_{11}$ at 353 K (a) and a type E alloy of $Ti_{45}V_{45}Ni_{10}$ at 523 K (b).

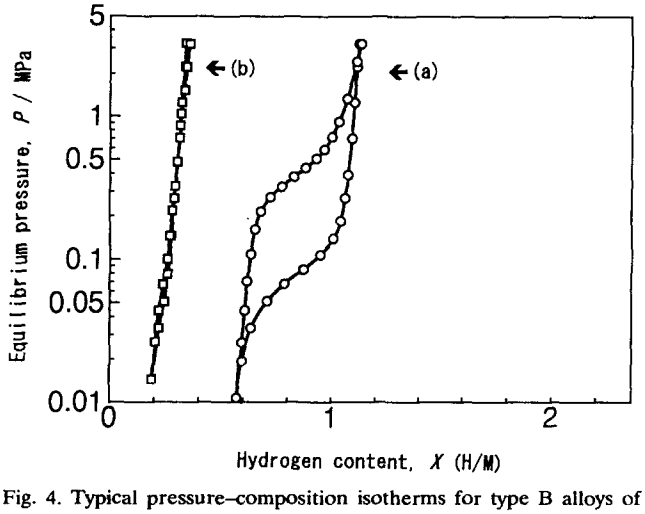

Fig. 4. Typical pressure–composition isotherms for type B alloys of $Ti_{10}V_{68}Ni_{22}$ at 353 K (a) and $Ti_{10}V_{60}Ni_{30}$ at 353 K (b).

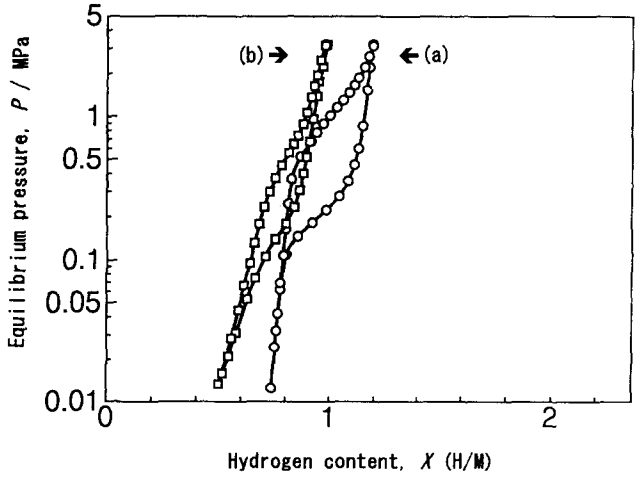

Fig. 6. Typical pressure–composition isotherms for type F alloys of $Ti_{21}V_{63}Ni_{16}$ at 313 K (a) and $Ti_{40}V_{40}Ni_{20}$ at 413 K (b).

type D alloy of $Ti_{22}V_{67}Ni_{11}$ (Ti/V = 0.33) in Fig. 5(a). Another type F alloy of $Ti_{40}V_{40}Ni_{20}$ showed a clearer plateau than $Ti_{50}V_{50}$ (type A, Fig. 3(b)) and $Ti_{45}V_{45}Ni_{10}$ (type E, Fig. 5(b)).

It was considered that the σ- or δ- or η-phase in the type B, D, E and F type alloys had no pressure plateau on PCT curves. The pressure plateau would be ascribed to the hydride formation of the β-phase.

In preliminary experiments, electrochemical PCT measurements of Ti–V alloys and Ti–V–Cr alloys were tried, but those alloys without nickel could not be activated electrochemically in KOH solution, although vanadium was reported to absorb hydrogen in phosphoric acid [16]. Adding nickel to the Ti–V alloy made it dischargeable as a metal–hydride electrode.

An electrochemical PCT curve for $Ti_{22}V_{66}Ni_{12}$ (the type D) is shown in Fig. 7, compared with the data obtained with the Sieverts' type apparatus. Two plateaus were observed by the electrochemical method at 10^{-2} MPa and 10^{-6} MPa in good agreement with the typical PCT curve reported for a group V metal-based bcc solid solution [3]. At 293 K the upper plateau would appear just under the lower limit of the pressure of the Sieverts' type apparatus. The equilibrium pressure for the upper plateau obtained by the electrochemical method would be the same as the equilibrium pressure obtained by the gas process. The upper plateau would correspond to the reaction from dihydride (MH_2) to monohydride (MH) as follows:

$$MH_2 \longrightarrow MH + \tfrac{1}{2}H_2$$

The lower plateau would be ascribed to the reaction of monohydride (MH) to metal (M) as follows:

$$MH \longrightarrow M + \tfrac{1}{2}H_2$$

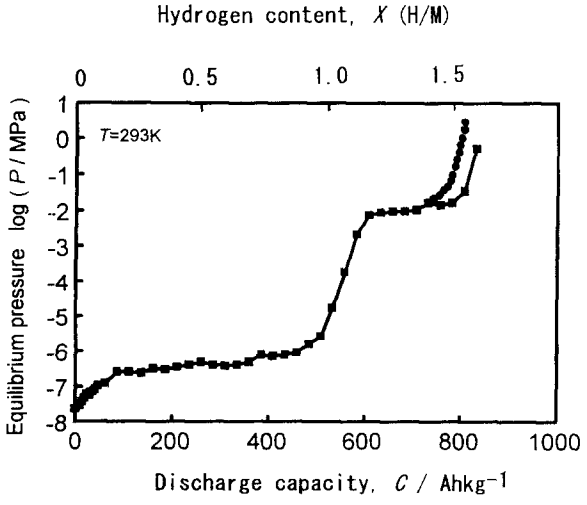

Fig. 7. Pressure–composition isotherm for $Ti_{22}V_{66}Ni_{12}$ at 293 K obtained by the electrochemical method (■) and with the Sieverts' type apparatus (●).

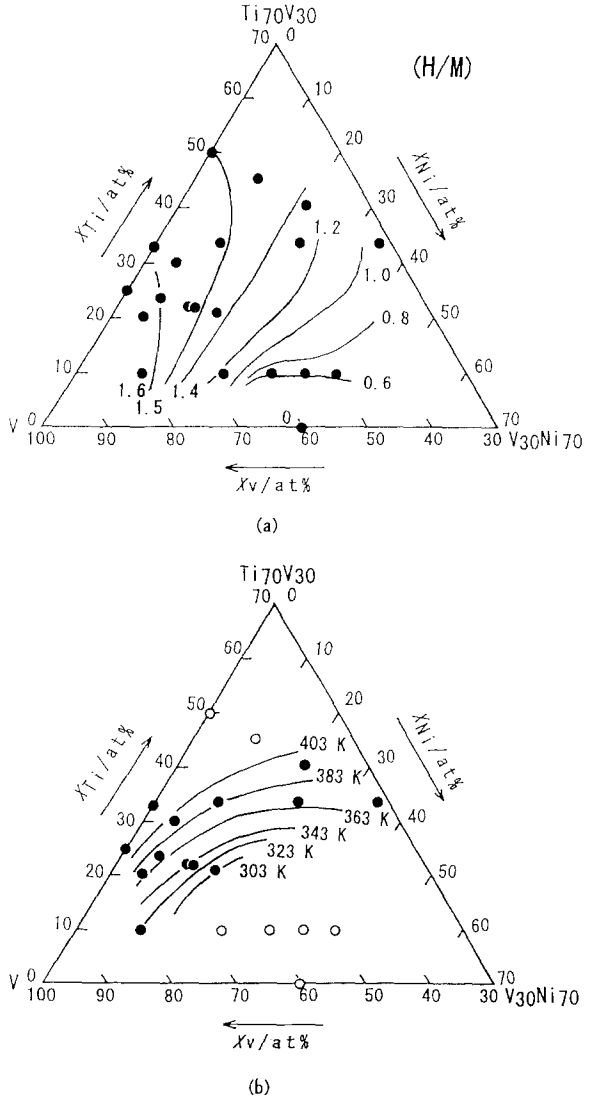

Fig. 8. Hydrogen storage capacity in H/M (a) and standard dissociation temperature (b) in Ti–V–Ni partial phase diagram. The symbol ● indicates the composition points of the samples that were used for plotting.

Vanadium is known to be easy to dissolve in the electrochemical process. The difference of 0.08 in H/M between the two PCT curves in Fig. 7 might be caused by the dissolution. This effect would not be significant for the PCT curve. The hydrogen storage capacity of $Ti_{22}V_{66}Ni_{12}$ was 3.2 mass% (about 800 $Ahkg^{-1}$) though the practical discharge capacity due to the reaction (2) would be about a half of this value. The equilibrium pressure of the lower plateau would be too low to dissociate hydrogen in practical use and measure the pressure with a conventional Sievert's type apparatus.

3.3. Hydrogen storage capacity and standard dissociation temperature

Fig. 8 shows the hydrogen storage capacity (a) and the standard dissociation temperature (SDT) (b) ob-

tained from the results of the PCT measurements. The hydrogen storage capacity was defined as a hydrogen content obtained at 293 K at 3.3 MPa hydrogen except for $Ti_{21}V_{63}Ni_{16}$ whose hydrogen storage capacity was determined at 253 K at 3.3 MPa hydrogen. The SDT was defined as the temperature when the hydrogen dissociation pressure reached 0.1 MPa and was determined by interpolating two PCT curves. The SDT values of σ-phase rich alloy and $(TiV)_{100-x}Ni_x$ ($x=0$, 10) were not given because the plateaus of those alloys were not clear enough to determine the SDT.

The hydrogen storage capacity decreased with increasing nickel content except for the region containing σ-phase (the type B and the type C). The alloy containing more than 85at.% vanadium showed a very high hydrogen storage capacity of 1.6 in H/M that amounted to 3.2 mass% hydrogen. The hydrogen storage capacity of the type B ($\beta+\sigma$) alloys depended mainly on titanium content.

The SDT depended on both nickel and titanium content. The SDT increased with increasing titanium content and decreased with increasing nickel content, depending on the size of the substitute elements in the main β-phase.

4. Conclusions

The solid solution type alloys of the Ti–V–Ni system were found to store a large amount of hydrogen (3.2 mass% hydrogen) whose value was considerably higher than those of AB_5 alloys (about 1 mass% hydrogen). The vanadium rich alloys in a wide composition range form the (βTi, V) based solid solution (β-phase) as a main phase, which absorbs a large amount of hydrogen. The hydrogen storage capacity and the standard dissociation temperature for these alloys decreases with increasing nickel content. The σ-phase rich alloys absorb much less hydrogen than the β-phase rich alloys.

The electrochemical PCT curve of $Ti_{22}V_{66}Ni_{12}$ was obtained with two pressure plateaus at 10^{-2} MPa and 10^{-6} MPa. The lower plateau pressure is too low to utilize the reaction for practical applications, but the alloy can still contain about 1.5 mass% reversible hydrogen.

References

[1] T. Schober and H. Wenzl, Hydrogen in Metals II, in G. Alefeld and J. Völkl (eds.), Springer–Verlag, Berlin, Heidelberg, 1978, *Topics in Applied Physics, vol. 29*, p. 11.

[2] K. Fujita, Y.C. Huang and M. Tada, *Nippon Kinzoku Gakkaishi, 43* (1979) 601.

[3] G.G. Libowitz and A.J. Maeland, *Mater. Sci. Forum, 31* (1988) 177.

[4] A.J. Maeland, T.R.P. Gibb, Jr. and D.P. Shumacher, *J. Am. Chem. Soc., 83* (1961) 3728.

[5] J.J. Reilly and R.H. Wiswall, *Inorg. Chem., 9* (1970) 1678.

[6] R.L. Zanowick and W.E. Wallace, *J. Chem. Phys., 36* (1962) 2059.

[7] T.B. Massalski (ed.), *Binary Alloy Phase Diagrams*, American Society for Metals, OH, 1986, vol. 2, p. 2134.

[8] T. Hagi, Y. Sato, M. Yasuda and K. Tanaka, *Trans. JIM., 28* (1987) 198.

[9] J.E. Kleiner, E.H. Sevilla and R.M. Cotts, *Phys. Rev. B33,* (1986) 6662.

[10] A.J. Maeland, G.G. Libowitz, J.F. Lynch and G. Rak, *J. Less-Common Met., 104* (1984) 133.

[11] A. Kagawa, E. Ono, T. Kusakabe and Y. Sakamoto, *J. Less-Common Met., 172* (1991) 64.

[12] T. Sakai, H. Yoshinaga, H. Miyamura, N. Kuriyama, A. Kato, K. Oguro and H. Ishikawa, *J. Alloys Comp., 180* (1992) 37.

[13] V.N. Eremenko, L.A. Tret'chenko, S.B. Prima and E.L. Semenova, *Soviet Powder Metallurgy and Metal Ceramics, 23* (1984) 613.

[14] T. Sakai, H. Miyamura, N. Kuriyama, A. Kato, K. Oguro, H. Ishikawa and C. Iwakura, *J. Less-Common Met., 159* (1990) 127.

[15] S. Ono, K. Nomura and Y. Ikeda, *J. Less-Common Met., 72* (1980) 159.

[16] H. Müller and K. Weymann, *J. Less-Common Met., 119* (1986) 115.